ISSN 1063-7745, Crystallography Reports, 2008, Vol. 53, No. 7, pp. 1157–1162. © Pleiades Publishing, Inc., 2008.

PHYSICAL PROPERTIES OF CRYSTALS

Optical Properties of Trigonal Single Crystals (Yb,Tm)$Al_3(BO_3)_4$ Grown from Fluxes Based on the Bismuth and Lithium Molybdates

V. L. Temerov, A. É. Sokolov, A. L. Sukhachev, A. F. Bovina, I. S. Édel'man, and A. V. Malakhovskiĭ

Kirensky Institute of Physics, Siberian Branch, Russian Academy of Sciences, Akademgorodok, Krasnoyarsk, 660036 Russia
e-mail: bezm@iph.krasn.ru

Received November 3, 2006

Abstract—The conditions for synthesis of $Yb_xTm_{1-x}Al_3(BO_3)_4$ ($x = 0$, 0.1, 0.2, 1.0) single crystals from fluxes based on bismuth trimolybdate $Bi_2Mo_3O_{12}$ and lithium molybdate Li_2MoO_4 are investigated. It is proposed to grow them by the group method on seeds. The polarized optical absorption spectra are measured for two mutually orthogonal linear polarizations at temperatures of 100 and 300 K.

PACS numbers: 78.20.-e, 78.40.Ha, 75.50.Ee

DOI: 10.1134/S1063774508070110

INTRODUCTION

In fabrication of high-efficiency materials for diode-pumped minilasers with frequency self-doubling (or up-conversion), single crystals of mixed rare earth borates $Y_{1-x-y}Yb_xTm_yAl_3(BO_3)_4$ with huntite structure are of great interest. To date, their optical and lasing characteristics have been most thoroughly studied only for single crystals with a relatively low concentration of one of the active substituents and grown from fluxes based on $K_2Mo_3O_{10}$ [1, 2].

The question of application and efficiency of $Y_{1-x-y}Yb_xTm_yAl_3(BO_3)_4$ single crystals with double yttrium substitution in up-conversion generation schemes remains open. Single crystals with extremely high concentrations of Yb ($x = 1$, $y = 0$) or Tm ($x = 0$, $y = 1$) are also of great interest as magneto-optical media [3].

In this study, to obtain $Yb_xTm_{1-x}Al_3(BO_3)_4$ single crystals, including ones with limiting concentrations of Yb and Tm, we investigated the conditions of their synthesis from fluxes based on bismuth trimolybdate $Bi_2Mo_3O_{12}$ and lithium molybdate Li_2MoO_4. A group method of their growth on seeds is proposed. The optical absorption spectra of the $Yb_xTm_{1-x}Al_3(BO_3)_4$ (x = 0, 0.1, 0.2, 1.0) single crystals grown by this method were measured for two mutually orthogonal linear polarizations at temperatures of 100 and 300 K.

CRYSTAL GROWTH CONDITIONS

To find fluxes appropriate for growing $Yb_xTm_{1-x}Al_3(BO_3)_4$ ($0 \le x \le 1$) single crystals with huntite ($CaMg_3(CO_3)_4$) structure (sp. gr. $R32$), we investigated the $Bi_2Mo_3O_{12} + pLiMoO_4 + qB_2O_3 + rYb_xTm_{1-x}Al_3(BO_3)_4$ system, similar to that used to obtain the trigonal phases (Tb,Er)(Fe,Ga)$_3(BO_3)_4$ [4].

Observation of the spontaneous nucleation and sequence of crystallizing phases revealed that this system is characterized by such a set of the coefficients p, q, and r in the ranges $0 \le p \le 1$, $0 \le q \le 3$, and $0.25 \le r \le 0.5$ that both ytterbium and thulium aluminum borates ($x = 1$ and 0, respectively) are high-temperature phases in the range 900–1000°C.

We chose the [100 – n] wt % [$Bi_2Mo_3O_{12} + pLiMoO_4 + qB_2O_3$] + n, wt % $Yb_xTm_{1-x}Al_3(BO_3)_4$ compositions with $n = 14$, $p = 0.75$, and $q = 2.5$ to grow $YbAl_3(BO_3)_4$ and with $n = 14$, $p = 0.5$, and $q = 2$ to grow $TmAl_3(BO_3)_4$, $Yb_{0.1}Tm_{0.9}Al_3(BO_3)_4$, and $Yb_{0.2}Tm_{0.8}Al_3(BO_3)_4$. The crystallization parameters for these fluxes were almost the same: specifically, the saturation temperature $T_{sat} \sim 985$°C, the concentration dependence of the saturation temperature dT_{sat}/dn = (12–15)°C/wt %, the width of the metastable zone ~20°C, and the crystallization range of $Yb_xTm_{1-x}Al_3(BO_3)_4$ near ~100°C. At an acceptable flux viscosity and a flux density not higher than the crystal density ($\rho_f < \rho_{cr}$), stable crystal growth was provided near the flux surface.

In each case, the flux with a total mass of 1 kg was prepared in a cylindrical platinum crucible (D = 100 mm, H = 90 mm) by successive alloying of ($Bi_2O_3 + MoO_3$), B_2O_3, ($Tm_2O_3 + Yb_2O_3 + Al_2O_3$), and ($Li_2CO_3 + MoO_3$) oxides at T = 1050–1100°C. Then the crucible with the prepared flux was placed in a crystallization furnace with a temperature field whose vertical component at T = 1000°C decreased with a gradient of

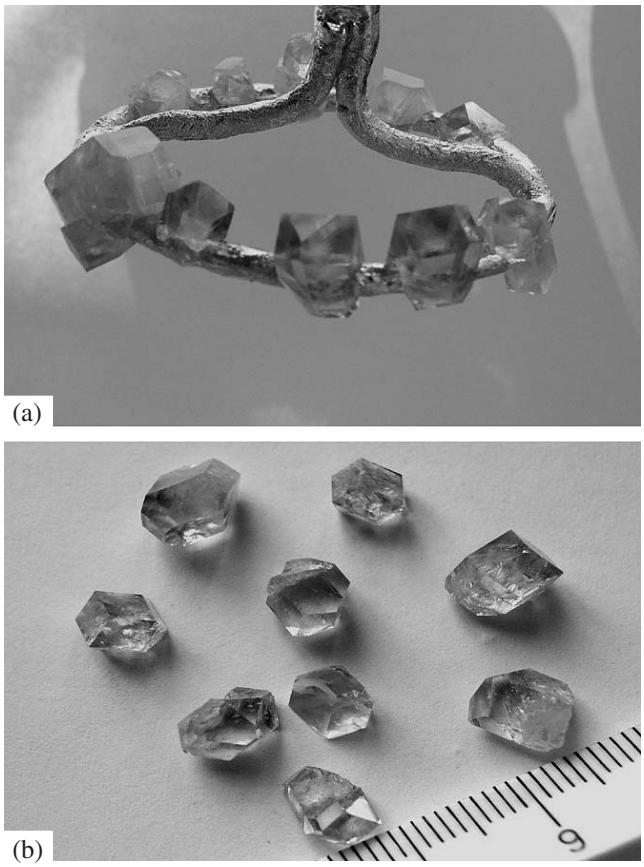

Fig. 1. (a) $YbAl_3(BO_3)_4$ and (b) $TmAl_3(BO_3)_4$ single crystals grown on prismatic and point seeds, respectively.

1–2°C with increasing distance from the crucible bottom. The flux was homogenized at $T = 1050$°C for 5–10 h, with a carrier immersed in the flux and rotated at $\omega = 30$ rpm (Fig. 1a). A preliminary search for the saturation temperature was performed by observing the formation of spontaneous microcrystallites on the carrier. After repeated homogenization, the value of T_{sat} was refined within ±2°C using the obtained microcrystallites (from the temperatures of their growth and dissolution).

Concerning control of crystal growth, the most favorable mode is the seed growth. Generally, 10–12 "point" seeds (microcrystallites of high structural quality about 1 mm^3 in size) or 6–8 prismatic seeds (rectangular prisms with a cross-sectional area of ~1 mm^2 and two lateral faces oriented parallel to the natural crystal face) were installed on the ring. When prismatic seeds were used, the growth efficiency increased owing to the increase in the initial growth surface.

Lattice parameters of the grown crystals

Crystal	Lattice parameters, Å	
	a	*c*
$TmAl_3(BO_3)_4$	9.280(1)	7.211(1)
$YbAl_3(BO_3)_4$	9.274(3)	7.212(3)

After determining T_{sat} and superheating the flux at $T = 1050$°C for 2–4 h, the carrier was suspended above the flux and the temperature in the furnace decreased to $T = T_{sat} + 7$°C. Then the carrier was immersed into the flux to a depth of 15–20 mm and reverse rotation (with a period of 1 min) at a rate of 30 rpm was switched on. After 15 min, the temperature decreased to the starting value, $T = T_{sat} - 10$°C, which corresponds to the middle of the metastable zone. Furthermore, the flux temperature gradually decreased at a programmably set rising rate (1–3°C/day), corresponding to crystal growth at a rate of no more than 1 mm/day. After the end of the growth process, the carrier was lifted above the flux and cooled to room temperature with the furnace supply switched off. During a 20-day cycle, the flux mass decreased owing to evaporation by no more than 3–4%. After replenishment of the fluxes with crystal-forming oxides in the amount corresponding to the mass of extracted crystals, the fluxes had T_{sat} close to initial and were used repeatedly.

A typical result obtained by growing $YbAl_3(BO_3)_4$ and $TmAl_3(BO_3)_4$ single crystals on prismatic and point

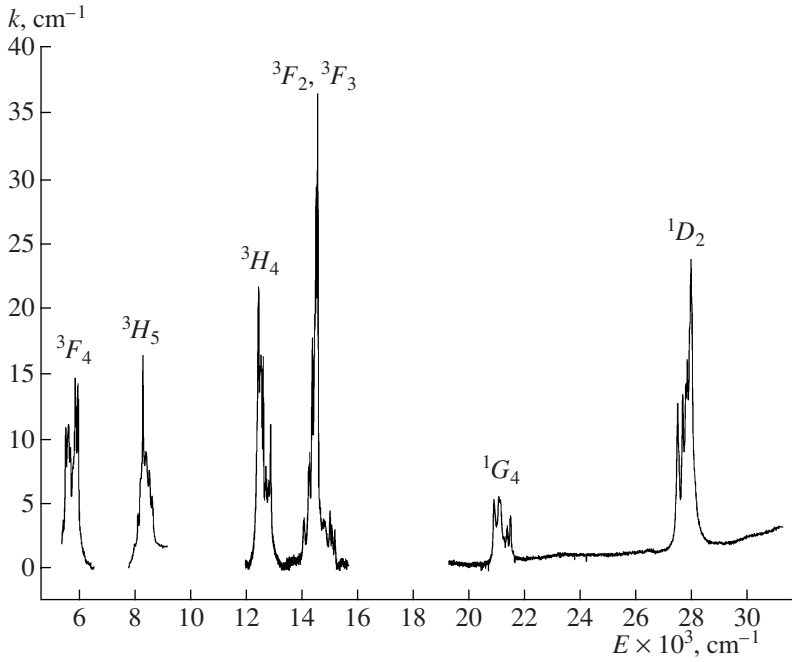

Fig. 2. Absorption spectrum of the $TmAl_3(BO_3)_4$ single crystal at room temperature (σ polarization).

seeds, respectively, is shown in Fig. 1. The former crystals are colorless, and the latter have a weak yellow-green hue. The shape of both Yb- and Tm-containing crystals grown on point seeds was close to isometric, and most of them had a small {0001} face. When prismatic seeds cut along the threefold axis were used, the grown crystals were extended in the same direction (Fig. 1a). Therefore, even in the absence of the {0001} face, their crystallographic orientation could be easily determined. The lattice parameters of the grown crystals are shown in the table.

ABSORPTION SPECTRA

The absorption spectra of $TmAl_3(BO_3)_4$, $YbAl_3(BO_3)_4$, $Yb_{0.2}Tm_{0.8}Al_3(BO_3)_4$, and $Yb_{0.1}Tm_{0.9}Al_3(BO_3)_4$ single crystals were recorded at 100 and 300 K in the wavelength range from 350 to 850 nm at two orientations of the samples with respect to the light wave vector: (i) the vector **E** of the light wave is parallel to the C_3 axis of the crystal (π polarization) and (ii) the vector **E** is perpendicular to the C_3 axis (σ polarization). The spectral resolution was ~10 cm^{-1}. An Ahrens prism was used as a polarizer.

Figure 2 shows the full-range absorption spectrum of $TmAl_3(BO_3)_4$ in the σ polarization. One can see the bands due to the electronic transitions from the ground state $^3H_6$ of Tm^{3+} ions to the excited states $^3F_4$, $^3H_5$, $^3H_4$, $^3F_2 + {}^3F_3$, $^1G_4$, and $^1D_2$. Previously, we have reported the room-temperature spectra of the bands due to the $^3H_6 \longrightarrow {}^3H_4$, $^3F_2 + {}^3F_3$ transitions [3]. There are data in the literature on the absorption spectra of Tm^{3+} impurity ions in a number of crystals: $GdAl_3(BO_3)_4$ [5], $KGd(WO_4)_2$ [6, 7], $SrGdGa_3O_7$ [8], and $SrWO_4$ [9]. The peak positions of the bands observed by us in the concentrated $TmAl_3(BO_3)_4$ crystal are close to the data of [5–9] for doped crystals. The distribution of band intensities is somewhat different for different crystal matrices. An especially strong difference in the relative intensities is observed for the bands due to the $^3H_6 \longrightarrow {}^1G_4$ and $^3H_6 \longrightarrow {}^1D_2$ transitions. In the case under consideration, the second band intensity is almost an order of magnitude higher, whereas, for Tm^{3+} impurity ions in all the crystals considered in [5–9], both bands have comparable intensities. It is noteworthy that, for doped crystals, both of these bands are observed on the wing of the strong absorption band, whose edge is in the range 320–350 nm (see, for example, [6, 7]). In the $TmAl_3(BO_3)_4$ crystal under study, the strong absorption edge is shifted by at least 220 nm. Thus, the proposed technology provides high crystal transparency in a wide UV range.

With a decrease in temperature, the thermal occupancy of the sublevels of the ground state of Tm^{3+} ions changes, resulting in a significant change in the structure of each band. The intensities of the lines due to the transitions from the upper sublevels of the ground state decrease, while the lines due to the transitions from the lower sublevels, on the other hand, become stronger. The band structure for the $^3H_6 \longrightarrow {}^1G_4$ and $^3H_6 \longrightarrow {}^1D_2$ transitions at 100 and 300 K is shown in Figs. 3a and 3b. A similar pattern is observed for the other bands.

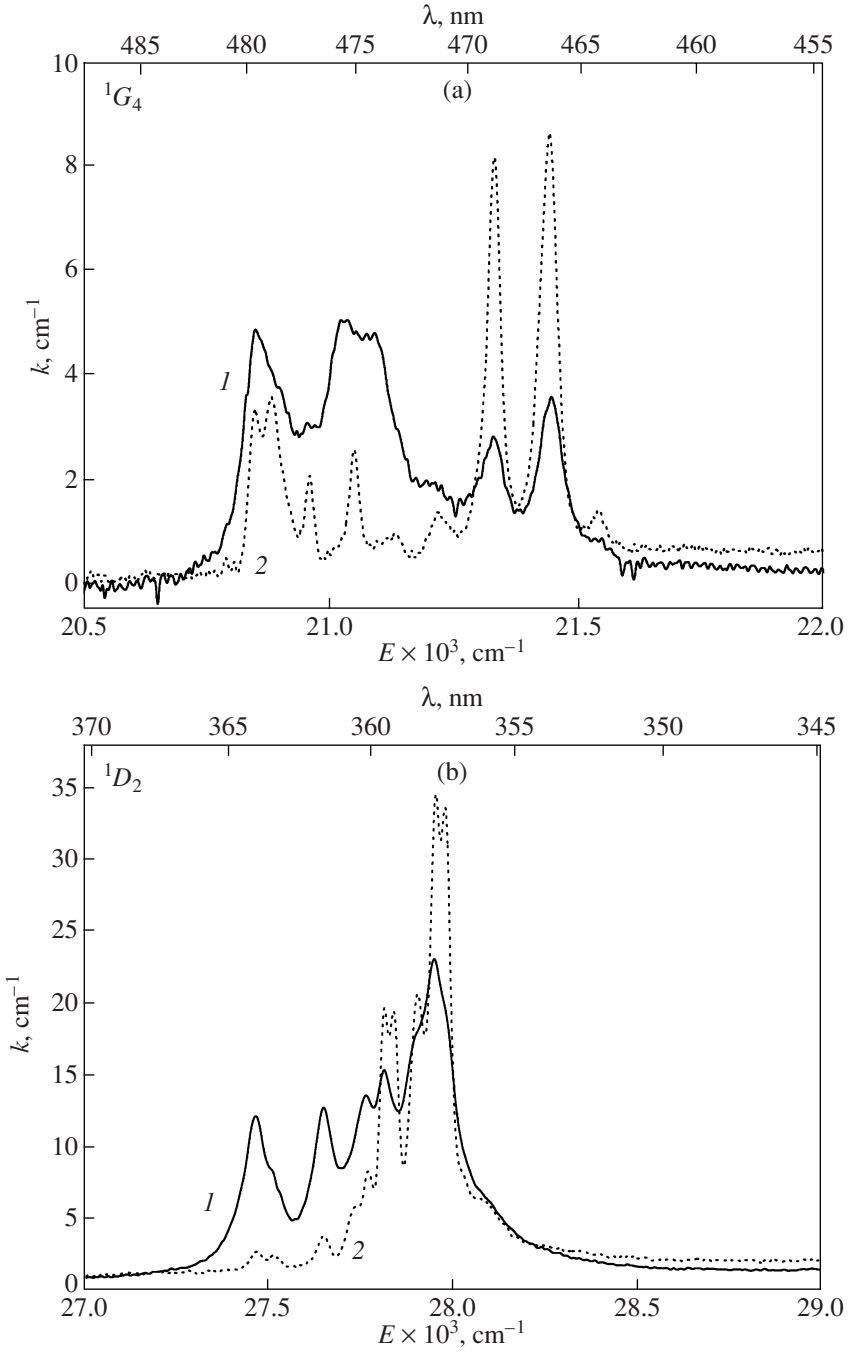

Fig. 3. (a) Absorption spectrum ($^3H_6 \longrightarrow {}^1G_4$ transition) of the $TmAl_3(BO_3)_4$ crystal at (*1*) 300 and (*2*) 100 K (σ polarization) and (b) the absorption spectrum ($^3H_6 \longrightarrow {}^1D_2$ transition) of the $TmAl_3(BO_3)_4$ crystal at (*1*) 300 and (*2*) 100 K (σ polarization).

Note that, for all observed absorption bands, the significant difference in the spectra recorded in π and σ polarizations manifests itself both in the difference in the integrated band intensities and in the intensity distribution over components. Some lines are observed only in the π polarization or only in the σ polarization. Characteristic examples are shown in Figs. 4a and 4b, which present the spectra for the $^3H_6 \longrightarrow {}^3F_2 + {}^3F_3$ and $^3H_6 \longrightarrow {}^3H_4$ transitions at 100 K, recorded in the σ and π polarizations.

In contrast to Tm^{3+} ions, Yb^{3+} ions undergo only one *f–f* transition ($^2F_{7/2} \longrightarrow {}^2F_{5/2}$) in the IR range near 950 nm. The absorption band due to this transition, which is between the $^3H_6 \longrightarrow {}^3H_5$ and $^3H_6 \longrightarrow {}^3H_4$ transitions in the Tm^{3+} ion, caused interest in the crystals including simultaneously these two ions in view of the

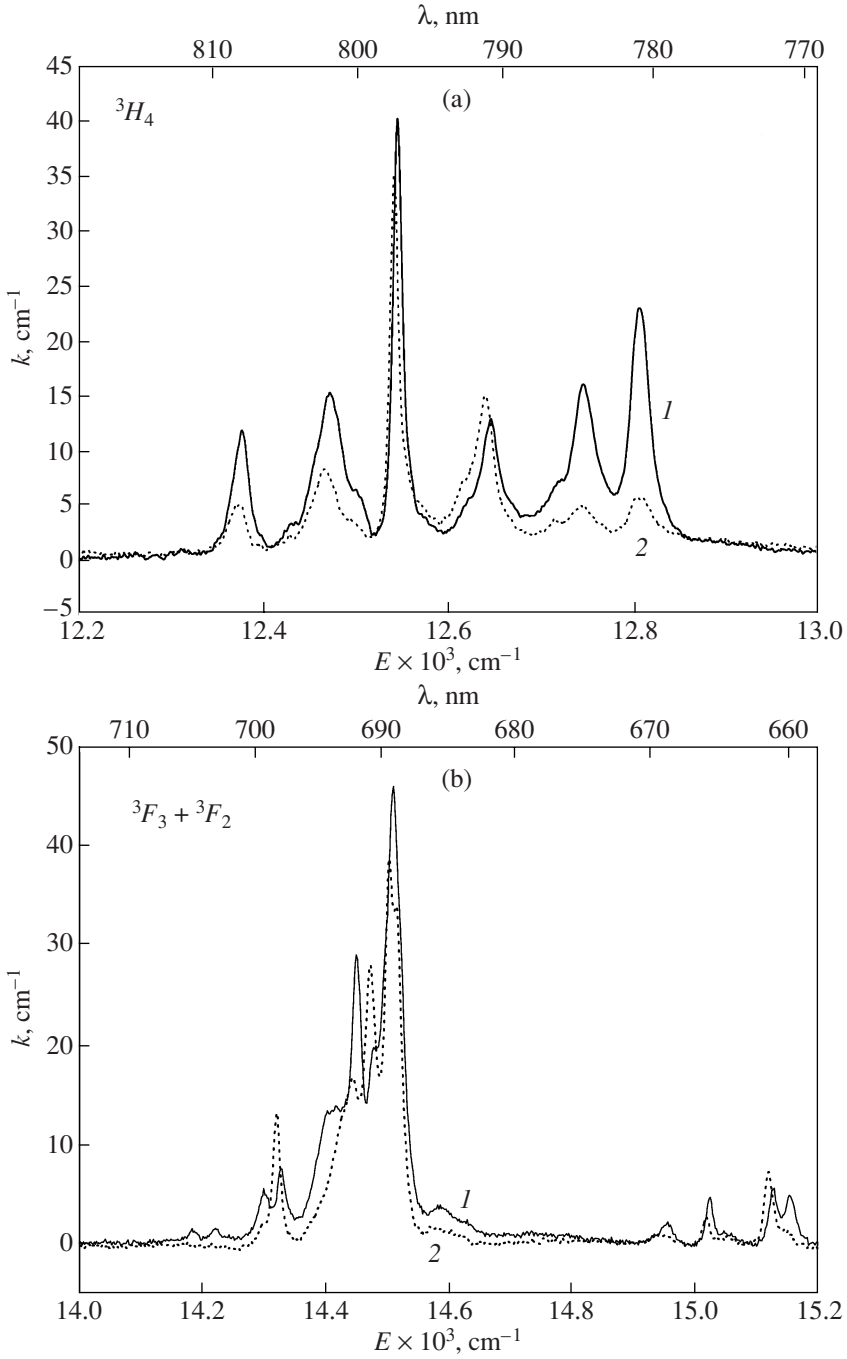

Fig. 4. (a) Absorption spectrum ($^3H_6 \longrightarrow {}^3F_3$ and $^3H_6 \longrightarrow {}^3F_2$ transitions) of the $TmAl_3(BO_3)_4$ crystal at 100 K (π and σ polarizations) and (b) the absorption spectrum ($^3H_6 \longrightarrow {}^3H_4$ transition) of the $TmAl_3(BO_3)_4$ crystal at 100 K (π and σ polarizations).

possibility of organizing an energy-transfer process. The optical spectrum of Yb^{3+} has been studied in both impurity and concentrated crystals [2, 10–12]. Figure 5 shows the molar extinction spectra of Yb^{3+}, recorded at 100 K for $Yb_{0.1}Tm_{0.9}Al_3(BO_3)_4$ and $Yb_{0.2}Tm_{0.8}Al_3(BO_3)_4$ crystals. The spectra of these crystals are similar, and the band integrated intensity is approximately proportional to the Yb concentration. However, the effect of the decrease in the Tm concentration with respect to the Yb concentration is pronounced; it manifests itself in the redistribution of the component intensities of the absorption band of Yb^{3+}. At $x = 0.1$, one might expect that the second coordination sphere of each Yb^{3+} ion is occupied by only Tm^{3+} ions; i.e., all Yb^{3+} ions have the same coordination. If the Yb concentration increases with respect to the Tm concentration, the second coordination sphere of Yb^{3+} ions will consist of not only

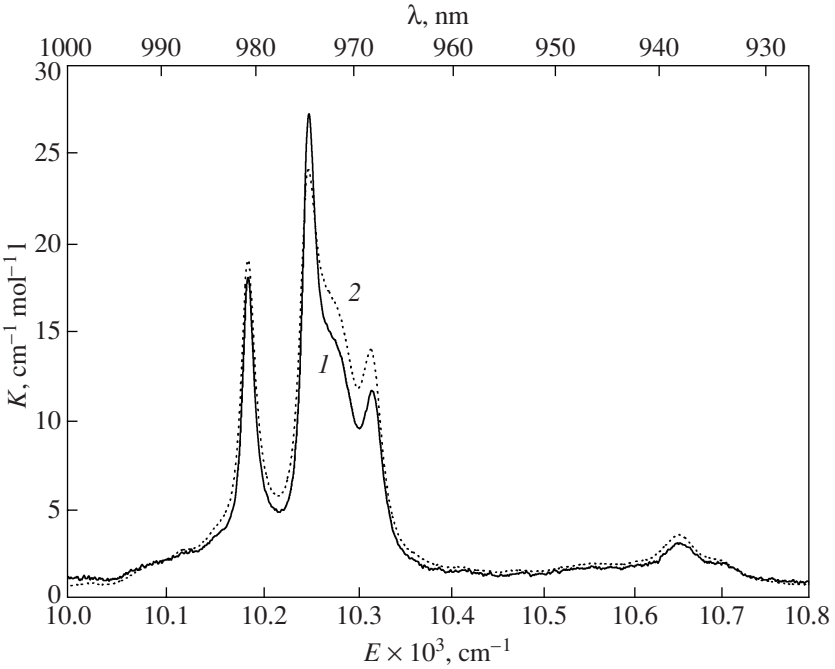

Fig. 5. Absorption spectra of the (*1*) $Yb_{0.1}Tm_{0.9}Al_3(BO_3)_4$ and (*2*) $Yb_{0.2}Tm_{0.8}Al_3(BO_3)_4$ crystals at 100 K (σ polarization) near the $^2F_{7/2} \longrightarrow {}^2F_{5/2}$ transition in Yb^{3+} ions.

Tm^{3+} ions with identical ionic radii but will include also Yb^{3+} ions with a smaller ionic radius, as a result of which the symmetry of the nearest environment of some part of Yb^{3+} ions will be distorted. Intraconfiguration *f–f* transitions are allowed owing to the noncentrosymmetric distortions of the crystal field. Therefore, they are very sensitive to changes in the nearest environment of active ions; specifically this effect was observed by us.

CONCLUSIONS

It is shown that the fluxes based on $Bi_2Mo_3O_{12}$–Li_2MoO_4, as media for growth of trigonal $Yb_xTm_{1-x}Al_3(BO_3)_4$ ($0 \le x \le 1$) single crystals, are superior to the fluxes based on potassium trimolybdate and other known fluxes [13, 14] in the main crystallization parameters and composition stability during long-term operation with an open crucible. A method of group growth of such crystals has been implemented. Polarized absorption spectra of the grown $Yb_xTm_{1-x}Al_3(BO_3)_4$ ($x = 0.0, 0.1, 0.2, 1.0$) crystals are reported.

ACKNOWLEDGMENTS

This study was supported in part by Grant NSh-4137.2006.2 of the President of the Russian Federation for Support of Leading Scientific Schools and the Russian Foundation for Basic Research (project no. 07-02-704). A.L. Sukhachev acknowledges the support of the Russian Science Support Foundation.

REFERENCES

1. J. Liao, Y. Lin, Y. Chen, et al., J. Cryst. Growth **267**, 134 (2004).
2. N. I. Leonyuk, E. V. Koporulina, V. V. Maltsev, et al., J. Cryst. Growth. **277**, 252 (2005).
3. A. V. Malakhovskiĭ, A. É. Sokolov, A. L. Sukhachev, et al., Fiz. Tverd. Tela (St. Petersburg) **49** (1), 32 (2007) [Phys. Solid State **49**, 34 (2007)].
4. L. N. Bezmaternykh, V. L. Temerov, I. A. Gudim, et al., Crystallogr. Rep. **50** (Suppl. 1), 97 (2005).
5. G. H. Lia, C. Yu. Tu, J. F. Li, et al., J. Appl. Phys. **96**, 6262 (2004).
6. F. Guell, X. Mateos, J. Gavalda, et al., Opt. Mater. **25**, 71 (2004).
7. Ch. Tu, J. Li, Zh. Zhu, et al., J. Cryst. Growth **256**, 63 (2003).
8. W. Ryba-Romanovsky, S Golab, I. Sokolska, et al., Appl. Phys. B **68**, 199 (1999).
9. G. Jia, Ch. Tu, Zh. You, et al., Solid State Commun. **134**, 583 (2005).
10. X. Xu, Z. Zhao, Ju. Xu, and P. Deng, J. Cryst. Growth **257**, 272 (2003).
11. A. Major, I. Nikolakakos, J. S. Aitchinson, et al., Appl. Phys. B **77**, 433 (2003).
12. A. Aron, G. Aka, B. Viana, et al., Opt. Mater. **16**, 181 (2001).
13. N. I. Leonyuk and L. I. Leonyuk, Prog. Cryst. Growth Charact. **31**, 179 (1995).
14. N. I. Leonyuk, Prog. Cryst. Growth Charact. **31**, 279 (1995).

Translated by Yu. Sin'kov